

Many-body Diagrammatic Expansion for the Exchange-Correlation Kernel in Time Dependent Density Functional Theory

I. V. Tokatly,* R. Stubner, and O. Pankratov

Lehrstuhl für Theoretische Festkörperphysik, Universität Erlangen-Nürnberg, Staudtstr. 7, 91058 Erlangen, Germany
(Dated: August 1, 2001)

A diagrammatic expansion for the dynamic exchange-correlation kernel f_{xc} of time dependent density functional theory is formulated. It is shown that f_{xc} has no singularities at Kohn-Sham transition energies in every order of the perturbation theory. However, it may diverge with the system size in extended systems. This signifies that any approximate perturbative substitute for f_{xc} requires a consistent perturbative treatment of the response function to avoid uncontrollable errors in the many-body corrections to excitations energies.

PACS numbers: 71.15.Mb, 31.15.Ew, 31.50.Df, 71.10.-w

The central problem of time dependent density functional theory (TDDFT)¹ is to find an adequate approximation for the dynamic exchange-correlation (xc) potential v_{xc} . In contrast to static DFT, where the local density approximation (LDA) has been extremely successful, no universal recipe for a dynamic v_{xc} has been found, and it remains unclear if such a recipe exists. The adiabatic LDA (ALDA), which is most popular in practical TDDFT calculations, is valid, by its nature, only in a quasistatic limit. This may suffice for a real-time dynamics of melting² or desorption³, but is hardly relevant for electronic excitations in insulators, where ALDA predicts the same erroneous band gaps as the static LDA.⁴ The improvement in excitation spectra of atoms and molecules which has been obtained in TDDFT using ALDA or the optimized effective potential (OEP) approximation is not indicative because in small systems the correction to the Kohn-Sham excitation energies is very small and approximations for f_{xc} play a secondary role in comparison to the accuracy of the static xc potential.^{5,6}

In general, electron-hole (e-h) excitation energies can be found as the poles of the density response function $\chi(\mathbf{r}, \mathbf{r}', \omega)$. TDDFT relates the exact $\chi(\omega)$ to the susceptibility of non-interacting Kohn-Sham (KS) particles $\chi_S(\omega)$ via the equation

$$\chi(\omega) = \chi_S(\omega) + \chi_S(\omega)\tilde{V}(\omega)\chi(\omega) \quad (1)$$

with $\tilde{V}(\omega) = V_C + f_{xc}(\omega)$, where V_C is the Coulomb potential and the xc kernel $f_{xc} = \delta v_{xc}(\mathbf{r}, t)/\delta n(\mathbf{r}', t')$ describes xc effects at the linear response level.⁷ Equation (1), which simultaneously accounts for the self-energy and the electron-hole correlations, may seem like an attractive alternative to the very laborious two-step approach involving a GW calculation for one-particle states with a subsequent solution of the Bethe-Salpeter (BS) equation for an e-h pair. Unfortunately, no approximation for f_{xc} is available which would be as efficient as LDA in the static DFT. In ALDA a time-dependent density is simply inserted in the LDA xc potential, and f_{xc} becomes an instantaneous point interaction, which is qualitatively different from a nonlocal and retarded xc kernel in systems with an energy gap. In fact, it is *a priori* not clear

whether f_{xc} allows any reasonable approximation, since its analytical properties in a non-homogeneous system are not known.

From the viewpoint of the standard many-body formalism $\tilde{V}(\omega)$ in Eq. (1) acts as a mass operator for the density propagator χ , similar to the self-energy $\Sigma = G_0^{-1} - G^{-1}$, with G and G_0 being interacting and non-interacting one-particle Green's functions. In contrast to the Green's function, Σ has no free-particle singularities in any order of the perturbation theory, as it contains only irreducible diagrams. Hence it allows perturbative approximations. Similarly, the introduction of the "density mass operator" $\tilde{V} = \chi_S^{-1} - \chi^{-1}$ is motivated only if the latter does not possess the e-h singularities, which are present in χ_S and any finite order approximation to χ .

In this paper we use the KS-based many-body diagrammatic technique of Ref. 8 to derive a perturbative expansion for f_{xc} . We find that the kernel is indeed regular at KS frequencies. Yet, caution must be exercised in applying perturbative approximations [such as OEP (Refs. 7,9)] for f_{xc} in large systems to avoid uncontrollable errors or even unphysical divergences.

We start with the equation which relates $\chi(\omega)$ to the proper polarizability $\tilde{\chi}$

$$\chi(\omega) = \tilde{\chi}(\omega) + \tilde{\chi}(\omega)V_C\chi(\omega). \quad (2)$$

It is convenient to split $\tilde{\chi}$ as $\tilde{\chi} = \chi_S + \pi_{xc}$ where the xc part π_{xc} can be represented as a series of graphs.⁸ The first-order contribution $\pi_{xc}^{(1)}$ and examples of the second-order corrections $\pi_{xc}^{(2)}$ are shown in Fig. 1, where solid and dashed lines stand for the KS Green's functions and the Coulomb interaction respectively. To the wiggled line is assigned the inverse KS susceptibility χ_S^{-1} . It describes the scattering of KS particles by the xc potential v_{xc} . By the definition of v_{xc} , these processes exactly compensate the change of the density due to the self energy insertions in every order of the perturbation theory.⁸

The graphical expansion of f_{xc} can be obtained from the relation $f_{xc} = \chi_S^{-1} - \tilde{\chi}^{-1}$ (Ref. 7), which follows from Eqs. (1) and (2). The formal expansion of this equation

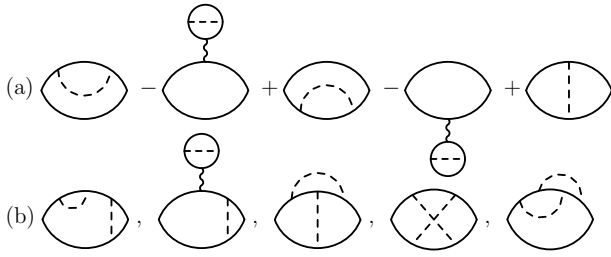


FIG. 1: (a) The first-order correction $\pi_{xc}^{(1)}$ to the proper polarizability; (b) examples of the second-order corrections

in terms of π_{xc} gives the series

$$f_{xc} = \chi_S^{-1} \pi_{xc} \chi_S^{-1} - \chi_S^{-1} \pi_{xc} \chi_S^{-1} \pi_{xc} \chi_S^{-1} \dots \quad (3)$$

Inserting $\pi_{xc} = \pi_{xc}^{(1)} + \pi_{xc}^{(2)} + \pi_{xc}^{(3)} + \dots$ and collecting the diagrams of the same order we obtain $f_{xc}^{(1)}$, $f_{xc}^{(2)}$, etc. The n -th order contribution $f_{xc}^{(n)}$ is a sum of the polarizability of the n -th order $\pi_{xc}^{(n)}$ with two attached wiggled lines and all diagrams with lower-order polarization loops connected by wiggled lines (Fig. 2). A closer inspection shows that all graphs with *internal* wiggled lines can be generated from a limited set of graphs with no internal but two *external* wiggled lines. This leads to the following rules for constructing $f_{xc}^{(n)}$: (i) Draw all standard diagrams¹⁰ for the proper polarization operator of the n -th order and attach wiggled lines to external points (construction of parent graphs). (ii) If possible, separate any given graph into two by cutting two fermionic lines. Join the external fermionic lines of these parts, connect them by a wiggled line and change the sign. Do not cut lines attached to the same wiggled line. (iii) Apply (ii) to all possible cuttings in all graphs, including those obtained previously. (iv) Keep only nonequivalent graphs. The arrows in Fig. 2 indicate application of these rules to the second-order parent graph in the upper left corner.¹⁴

The same rules apply to the perturbation series for the “mass operator” \tilde{V} , except that in (i) the parent graphs are the diagrams for the total response function χ . As discussed above, the introduction of \tilde{V} (or f_{xc}) is justified only if this function is free of singularities related to the

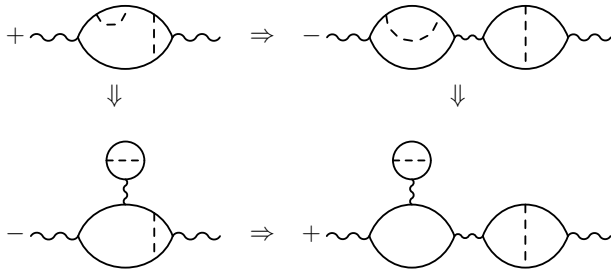


FIG. 2: Examples of the second-order graphs for f_{xc} . The arrows indicate an application of the rules (ii)-(iv) to the parent graph displayed in the upper left corner.

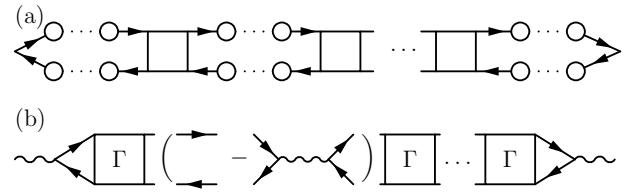


FIG. 3: (a) General graph of the L -th order for the response function χ ; (b) the diagram for the effective interaction which is produced from the general parent graph without self-energy insertions.

KS e-h pairs in every order of the perturbation theory. The analogy with the self-energy Σ does not, by itself, ensure this property, and we apply our graphical method to prove that this is indeed the case.

Since the rules (ii)-(iv) deal only with the two-particle reducible graphs, a partial summation of the diagrams with the help of one- and two-particle irreducible elements (self-energies and vertices) is possible. An example of a summation of all parent graphs with l vertex insertions (which divide each graph in $l + 1$ blocks) and with m_k ($k = 1, \dots, l + 1$) self-energies in every block is depicted in Fig. 3a. It is important that the diagrams generated by cutting two fermionic lines with the same frequency (e.g. in Fig. 1 and Fig. 2) have a similar structure. They all describe scattering of KS particles by the xc potential. The sum of these graphs and the parent graphs is again a diagram of the same type as in Fig. 3a with the self-energy $\Sigma_S = G_S^{-1} - G^{-1}$. This definition of Σ_S ensures the equivalence of the KS and exact densities. The vertex Γ is defined in the usual way as the sum of the four-point functions which are irreducible in the e-h channel. After summation, the graph in Fig. 3a can be considered as a new parent graph which generates further diagrams for \tilde{V} via cutting only parallel e-h lines.

Let us now consider the general parent graph of Fig. 3a at KS frequency $\omega_{ij} = E_i - E_j$, where E_j are the KS one-particle energies. This graph represents a L -th order correction (i.e. containing L irreducible elements) to the response function χ . When the frequency ω approaches ω_{ij} , the graph in Fig. 3a diverges. Integrating over intermediate frequencies in every internal block we find that the most divergent term behaves as $1/(\omega - \omega_{ij})^{(L+1)}$. Application of our rules to the graph Fig. 3a generates a full set of diagrams for $\tilde{V}(\omega)$ i.e. the initial graph with only two external wiggled lines and the diagrams obtained by all possible cuttings of parallel e-h lines. All diagrams in this set have poles of various orders. However, they can be grouped in such a way that all singularities cancel. The general proof is straightforward but lengthy and will be published elsewhere. Here we show this cancellation for a graph with L vertices, but with no self-energy insertions.

Application of the rules (i)-(iv) to this graph leads to replacement of all internal KS two-particle functions

$$K_S(\omega, \varepsilon) = G_S(\omega + \varepsilon)G_S(\varepsilon) \text{ by}$$

$$J(\omega, \varepsilon, \varepsilon') = K_S(\omega, \varepsilon)\delta_{\varepsilon, \varepsilon'} - K_S(\omega, \varepsilon)\chi_S^{-1}(\omega)K_S(\omega, \varepsilon'),$$

where ω and ε are transferred (external) and internal frequencies respectively. The resulting contribution to \tilde{V} is shown graphically in Fig. 3b. The singularities at $\omega = \omega_{ij}$ can potentially occur in the ‘‘resonant’’ part in every internal block $J_{ij}(\omega, \varepsilon, \varepsilon')$, which contains an electron in the state i and a hole in the state j . A summation over internal frequency gives for the ‘‘dangerous’’ contribution

$$\sum_{\varepsilon, \varepsilon'} J_{ij}(\omega, \varepsilon, \varepsilon') = \frac{|ij\rangle\langle ij|}{\omega - \omega_{ij}} - \frac{|ij\rangle\{ij\}}{\omega - \omega_{ij}}\chi_S^{-1}(\omega)\frac{|ij\rangle\langle ij|}{\omega - \omega_{ij}}, \quad (4)$$

where $|ij\rangle = \psi_i(\mathbf{r})\psi_j^*(\mathbf{r}')$ is the wave function of the resonant e-h pair, $\{ij\} = \psi_i(\mathbf{r})\psi_j^*(\mathbf{r})$ is the same function, but with equal coordinates of the electron and the hole and $\psi_i(\mathbf{r})$ are the KS orbitals. Both terms in Eq. (4) are apparently singular. To show that these divergences cancel, we single out the divergence in the KS susceptibility $\chi_S = |ij\rangle\{ij\}/(\omega - \omega_{ij}) + \chi_r$, where χ_r is the regular part. For the inverse $\chi_S^{-1}(\omega)$ we have

$$\chi_S^{-1}(\omega) = \chi_r^{-1}(\omega) - \frac{\chi_r^{-1}(\omega)|ij\rangle\{ij\}}{\omega - \omega_{ij} + \{ij|\chi_r^{-1}(\omega)|ij\rangle}. \quad (5)$$

Substitution of Eq. (5) to Eq. (4) gives a singularity-free result

$$\sum_{\varepsilon} J_{ij}(\omega_{ij}, \varepsilon) = \frac{|ij\rangle\langle ij|}{\{ij|\chi_r^{-1}(\omega_{ij})|ij\rangle}. \quad (6)$$

Similarly, zeroes of the external wiggled lines cancel the poles of the end blocks in Fig. 3b.¹⁵ Thus the graph Fig. 3b is regular at KS resonances in every order of the perturbation theory, and $\tilde{V}(\omega)$ can be viewed as a mass operator similar to the one-particle self energy Σ . There is, however, one important difference. Whereas the self energy exactly reduces to the one-particle irreducible elements, the effective interaction $\tilde{V}(\omega)$, even after cancellation of singularities, still contains parts of the bare two-particle propagator with the resonant denominator being replaced by $\{ij|\chi_r^{-1}(\omega_{ij})|ij\rangle$ (see Eq. (6)). Since $\chi_r^{-1}(\mathbf{r}, \mathbf{r}')$ in general goes to zero at $|\mathbf{r} - \mathbf{r}'| \rightarrow \infty$ and the functions $|ij\rangle$ have a normalization factor $\sim 1/V$, the matrix element $\{ij|\chi_r^{-1}|ij\rangle$ may vanish with the increase of the system size. For example, in a 3D semiconductor the inverse of the KS response function at $\omega = E_g$ has an asymptotic behavior $\chi_r^{-1}(E_g, \mathbf{r}, \mathbf{r}') \sim 1/|\mathbf{r} - \mathbf{r}'|$ (in this case χ_r means the principal value of χ_S). Therefore the matrix element $\{cv|\chi_r^{-1}(E_g)|cv\rangle$ vanishes as $V^{-1/3}$. This makes it problematic to construct approximations for f_{xc} using perturbation theory, as is routinely done for Σ .

The simplest of the perturbative approximations corresponds to the first order in irreducible elements Σ_S and Γ (Fig. 4a), $\tilde{V}^{(1)} = \chi_S^{-1}\chi^{(1)}\chi_S^{-1}$, where $\chi^{(1)}$ is the first-order polarization loop. This class of approximations covers, for instance, the dynamic x-only OEP

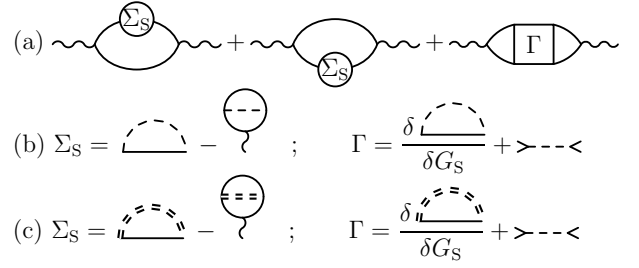


FIG. 4: (a) Graphical representation of the general first-order approximation $\tilde{V}^{(1)}$ to the effective interaction; (b) self-energy Σ_S and irreducible vertex Γ for OEP; (c) Σ_S and Γ for RA approximation. The double dashed line stands for the screened Coulomb interaction.

(Ref. 9) and the Richardson-Ashcroft approximation (RA).¹¹ $\tilde{V}_{OEP}(\omega)$ is given by the graph of Fig. 4a with Σ_S and Γ taken in the first order in the Coulomb interaction V_C (Ref. 8) in Fig. 4b. Similarly, $\tilde{V}_{RA}(\omega)$ has the same form of Fig. 4a, but with the self-energy Σ_S and the vertex Γ as shown in Fig. 4c. OEP and RA are state-of-the-art approximations which accurately reproduce the correlation energy and plasma excitations of a homogeneous electron gas.¹² However, both approximations may give uncontrollable results for the e-h excitation energies. In the following we show this by an explicit calculation of the second-order correction to the KS excitation energy ω_{ij} .

The first-order (with respect to Σ_S and Γ) correction $\Delta\omega_{ij}^{(1)} = \omega_{ij}^{(1)} - \omega_{ij}$ is given by

$$\Delta\omega_{ij}^{(1)} = \{ij|\tilde{V}^{(1)}(\omega_{ij})|ij\rangle \equiv \langle ij|\hat{W}|ij\rangle, \quad (7)$$

where the operator $\hat{W}(\mathbf{r}_1, \mathbf{r}'_1; \mathbf{r}_2, \mathbf{r}'_2)$ is defined as follows

$$\hat{W} = \Sigma_S^e(\mathbf{r}_1, \mathbf{r}_2)\delta(\mathbf{r}'_1 - \mathbf{r}'_2) - \Sigma_S^h(\mathbf{r}'_1, \mathbf{r}'_2)\delta(\mathbf{r}_1 - \mathbf{r}_2) + \Gamma^{eh}(\mathbf{r}_1, \mathbf{r}'_1; \mathbf{r}_2, \mathbf{r}'_2). \quad (8)$$

The upper indexes in Eq. (8) indicate that the self-energies and the vertex are taken on the e-h mass shell. The equations (7)-(8) give a generalization of the x-only result,⁸ which is equivalent to the first-order of the Görling-Levy perturbation theory.¹³

Similarly we obtain the second-order correction

$$\Delta\omega_{ij}^{(2)} = \{ij|\tilde{V}^{(2)}(\omega_{ij})|ij\rangle + \Delta\omega_{ij}^{(1)}\{ij|\frac{\partial\tilde{V}^{(1)}}{\partial\omega}|ij\rangle + \sum_{k,l \neq i,j} \frac{\{ij|\tilde{V}^{(1)}(\omega_{ij})|kl\rangle(n_k - n_l)\{kl|\tilde{V}^{(1)}(\omega_{ij})|ij\rangle}{\omega_{ij} - \omega_{kl}} \quad (9)$$

where n_k is the occupation number of the k -th KS state and $\tilde{V}^{(2)}(\omega)$ is the effective interaction of the second order in Σ_S and Γ . If we ignore $\tilde{V}^{(2)}$ and iteratively solve Eq. (1) using only the first-order function $\tilde{V}^{(1)}$ (e.g. in OEP or RA approximation) in place of the kernel, the second-order correction Eq. (9) would contain only the

last two terms. The last term can be written as

$$\{ij|\tilde{V}^{(1)}(\omega_{ij})\chi_r(\omega_{ij})\tilde{V}^{(1)}(\omega_{ij})|ij\} = \frac{(\Delta\omega_{ij}^{(1)})^2}{\{ij|\chi_r^{-1}(\omega_{ij})|ij\}},$$

where we used Eq. (7) and Eq. (5). A similar calculation of the second term in Eq. (9) shows that it contains the same factor $\{ij|\chi_r^{-1}|ij\}^{-1}$. Hence both terms in Eq. (9) which originate from $\tilde{V}^{(1)}$, and which would be the only contributions in OEP and RA, have exactly the same denominator as the higher-order diagrams after the cancellation of the e-h singularities (see Eq. (6)). Clearly this denominator must appear in $\tilde{V}^{(2)}$ as well. The calculation shows that the first term in Eq. (9) indeed takes the form

$$\begin{aligned} \{ij|\tilde{V}^{(2)}(\omega_{ij})|ij\} &= \Delta_{ij}^{(2)} - \Delta\omega_{ij}^{(1)}\{ij|\frac{\partial\tilde{V}^{(1)}}{\partial\omega}|ij\} \\ &- \{ij|\tilde{V}^{(1)}(\omega_{ij})\chi_r(\omega_{ij})\tilde{V}^{(1)}(\omega_{ij})|ij\}, \end{aligned} \quad (10)$$

where

$$\Delta_{ij}^{(2)} = \sum_{k,l \neq ij} \frac{\langle ij|\hat{W}|kl\rangle\langle kl|\hat{W}|ij\rangle}{\omega_{ij} - \omega_{kl}} + \Delta\omega_{ij}^{(1)}\{ij|\frac{\partial\hat{W}}{\partial\omega}|ij\}. \quad (11)$$

The second and the third terms in Eq. (10) cancel the second and the third terms in Eq. (9) and the second-order

energy shift is simply given by Eq. (11). This also follows from a direct perturbative solution of the BS equation. The cancellation found above is not accidental and can be proven in every order of the perturbation theory.

Thus any finite-order approximation for \tilde{V} requires a consistent perturbative treatment of Eq. (1) to obtain a meaningful energy shift. In particular, the first-order approximations like OEP or RA are appropriate for the calculation of the excitation energies only in the first order in Σ_S and Γ . The naive second-order correction, (last two terms in Eq. (9)) and higher-order corrections are wrong and can even diverge in extended systems. A summation of all orders (exact solution of Eq. (1)) may produce a finite result, but it will contain uncontrollable errors. In recent TDDFT calculations for atoms it has been indeed observed that exact (in contrast to perturbative) solution of Eq. (1) does not necessarily improve the results.⁵

This work has been supported by the Deutsche Forschungsgemeinschaft under Grant PA 516/2-1. O. P. is grateful for a partial support from the U.S. Department of Energy, Office of Basic Energy Sciences, Division of Materials Science by the University of California Lawrence Livermore National Laboratory under contract No. W-7405-Eng-48. The work of I. T. was partly supported by the Russian Federal Program "Integration".

* e-mail: ilya.tokatly@physik.uni-erlangen.de; on leave from Moscow Institute of Electronic Technology, Zelenograd, 103498, Russia; 99]

¹ E. Runge and E. K. U. Gross, Phys. Rev. Lett. **52**, 997 (1984).

² J. Theilhaber, Phys. Rev. B **46**, 12990 (1992).

³ Y. Miyamoto and O. Sugino, Phys. Rev. B **62**, 2039 (2000).

⁴ F. Kootstra, P. L. de Boeij, and J. G. Snijders, J. Phys. Chem. **112**, 6517 (2000).

⁵ M. Petersilka, E. K. U. Gross, and K. Burke, Int. J. Quantum Chem. **80**, 534 (2000).

⁶ M. E. Casida and D. R. Salahub, Journ. Chem. Phys. **113**, 8918 (2000).

⁷ M. Petersilka, U. J. Gossmann and E. K. U. Gross, Phys. Rev. Lett. **76**, 1212 (1996).

⁸ I. V. Tokatly and O. Pankratov, Phys. Rev. Lett. **86**, 2078 (2001).

⁹ A. Görling, Int. J. Quant. Chem. **69**, 265 (1998).

¹⁰ E. M. Lifshitz, L. P. Pitaewski, *Statistical Physics, Part 2*, Course of Theoretical Physics, Vol. 9 (Pergamon, New

York, 1980).

¹¹ C. F. Richardson and N. W. Ashcroft, Phys. Rev. B **50**, 8170 (1994).

¹² M. Lein, E. K. U. Gross and J. P. Perdew, Phys. Rev. B **61**, 13431 (2001); K. Tatarczyk, A. Schindlmayr and M. Scheffler, Phys. Rev. B **63**, 235106 (2001).

¹³ A. Görling, Phys. Rev. A **54**, 3912 (1996).

¹⁴ Interestingly, the rules (ii)-(iv) coincide with the diagrammatic rules for the xc potential v_{xc} (Ref. 8). The only difference is the choice of the parent graphs in (i) (loops with one or two external points for v_{xc} and f_{xc} respectively). This by far nontrivial fact leads to the conjecture that these rules should hold for any functional derivative $\delta^m E_{xc}/\delta n^m$ of the xc energy E_{xc} .

¹⁵ To simplify the derivation we assumed that the resonant transition ω_{ij} is not degenerate. In the case of M -fold degeneracy, the denominator in Eq. (6) is replaced by the inverse of the $M \times M$ matrix $\{ij|\chi_r^{-1}|i'j'\}$, where $|ij\rangle$ and $|i'j'\rangle$ belong to the set of degenerate states.